TISSUE ENGINEERING: Part A
Volume 16, Number 12, 2010

DOI: 10.1089/ten.tea.2010.0219

Microcavitary Hydrogel-Mediating Phase Transfer Cell Culture for Cartilage Tissue Engineering

Yihong Gong, Ph.D.,[1,2,*] Kai Su, B.Eng.,[1,*] Ting Ting Lau, B.Eng.,[1] Ruijie Zhou, B.Sc.,[1] and Dong-An Wang, Ph.D.[1]

Hydrogels have been widely used as cell-laden vehicles for therapeutic transplantation in regenerative medicine. Although the advantages of biocompatibility and injectability for *in situ* grafting have made hydrogel a superior candidate in tissue engineering, there remain challenges in long-term efficacy of tissue development using hydrogel, especially when more sophisticated applications are demanded. The major bottleneck lies in environmental constraints for neo-tissue generation in the gel bulk such as proliferation of encapsulated cells (colonies) *per se* and also accommodation of their endogenously produced extracellular matrices. In this study, we endeavor to develop an innovative tissue engineering system to overcome these drawbacks through a novel microcavitary hydrogel (MCG)-based scaffolding technology and a novel phase transfer cell culture (PTCC) strategy to enable phenotypically *bona fide* neo-tissue formation in an injectable artificial graft. For this purpose, microspherical cavities are created in cell-encapsulating hydrogel bulk via a retarded dissolution of coencapsulated gelatin microspheres. Based on proliferation and affinity selection, the encapsulated cell colonies adjacent to the gel-cavity interface will spontaneously outgrow the hydrogel phase and sprout into cavities, enabling neo-tissue islets to fill up the voids and further expand throughout the whole system for full tissue regeneration. The design of MCG-PTCC strategy was elicited from an observation of a spontaneous dynamic outgrowth of chondrocytes from the edge of a cell-laden hydrogel construct over prolonged cultivation—a phenomenon named edge flourish. This MCG-PTCC strategy potentially introduce a new application to hydrogels in the field of regenerative medicine through elevation of its role as a cell vehicle to a three-dimensional transplantable growth-guiding platform for further development of newly generated tissues that better fulfill the demanding criteria of scaffolds in therapeutic tissue regeneration.

Introduction

Bodies of organisms are mostly made of hydrogels that vary in diverse forms.[1,2] Therefore, the close mimicking of gel-like materials to our native tissue has led to extensive research of hydrogels in biomedical engineering in the past decades.[3–7] Other than hydrogels, there are several types of scaffolds also being used in tissue engineering applications: one of which is the plastic/protein porous sponge of poly(lactic-*co*-glycolic acid)[8] or collagen,[9] whereas another is the electrospun fibrous scaffold.[10,11] In both porous sponge and fibrous scaffolds, cells are seeded after scaffold formation and do not have injectability. Besides, these scaffolds induce cellular focal adhesion, which is not appropriate for articular hyaline cartilage regeneration.

The conventional hydrogel has the advantage of injectability, thus allowing *in situ* tissue development. Hence, much work has been focused on functionalizing hydrogels to enhance cell conveyance and accommodation,[12–15] but the breakthrough of hydrogel applications in the field of regenerative medicine is still impeded by limited cell growth and scarce tissue formation.[16,17] These constraints originate from two material-based backgrounds: (1) how to synchronize scaffold degradation with neo-tissue growth, which is a common challenge to most biodegradable scaffolds applied in the current tissue engineering systems[18–24]; and (2) how to provide cell adhesive moieties due to the intrinsic hydrophilic nature of the hydrogels, which has substantially hindered cellular development.[25–27]

Accordingly, to overcome both spatial limitations and deficiency of cell adhesive moieties for the engineered neotissues while still conserving all the beneficial properties of hydrogels such as injectability, we have designed a novel microcavitary hydrogel (MCG) model. The model is an inspiration from an observation of dynamic outgrowth of chondrocytes at the gel edge of conventional cell-laden

[1]Division of Bioengineering, School of Chemical and Biomedical Engineering, Nanyang Technological University, Singapore, Singapore.
[2]Guangzhou Higher Education Mega Center, School of Engineering, Sun Yat-Sen University, Guangzhou, China.
*These two authors contributed equally to this work.

hydrogel system and this phenomenon of active proliferation of cells and extracellular matrix (ECM) secretion at the gel edge is hence named edge flourish (EF) as illustrated in Figure 1. Based on this EF phenomenon, we have developed the MCG model. It aims to utilize spontaneous formation of microspherical cavities to introduce multiple gel edges into the hydrogel bulk, thereby promoting and accommodating the outgrowth of the proliferating cells/colonies from the cell-encapsulating gel phase to the microcavities—an unconfined phase just like the EF phenomenon. The whole strategy is therefore named phase transfer cell culture (PTCC).

Comparing our MCG-PTCC system with conventional porous scaffolds such as poly(lactic-*co*-glycolic acid) or collagen sponges or gels where cells could only be seeded after scaffold formation, our system coencapsulates both cells and 10^2-μm-scaled porogens simultaneously during scaffold fabrication, which not only ensures nearly full cell loading efficiency but also maintains injectability of the whole system. With this invention, we endeavor to transform the traditional role of hydrogel bulk from a mere cell vehicle to an integration of microincubators that physically direct and accommodate the growth of neo-tissue inside. In this study, cartilaginous system is chosen as an executive model system because chondrocytes are one of the non(typical) anchorage-dependent cells that could maintain viability within the noncell-adhesive hydrogel environment.

Materials and Methods

Chondrocytes isolation, encapsulation, and EF determination

Chondrocytes were isolated from cartilage tissues of porcine articular cartilage. One biopsy was done on one pig, and cells obtained in each biopsy were used for one experiment only. Altogether, six repeats were performed using six different pigs. Briefly, cartilage tissues obtained from the joint of 5-month-old pigs were cut into small chips. Chondrocytes were isolated by incubating the cartilage pieces in Dulbecco's modified Eagle's culture medium with 10% (v/v) fetal bovine serum containing 1 mg/mL collagenase type II at 37°C for 12 h under gentle stirring. The chondrocytes were then centrifuged and resuspended in chondrocytes culture medium, which is comprised of Dulbecco's modified Eagle's medium supplemented with 20% (v/v) fetal bovine serum, 0.01 M 4-(2-hydroxyethyl)-piperazine-1-ethanesulfonic acid, 0.1 mM nonessential amino acids, 0.4 mM proline, 0.05 mg/mL vitamin C, 100 units/mL penicillin, and 100 mg/mL streptomycin. The cell suspension was then seeded in 75 mL tissue culture flask (Falcon; seeding density: 2×10^4 cells/cm^2) and incubated in humidified air with 5% CO_2 at 37°C for routine culture. In this study, passage 1 cells were employed.

To demonstrate the EF phenomenon, chondrocytes were suspended at high density in gel precursor solution (in phosphate-buffered saline [PBS], agarose 0.02 g/mL; cell density: 1×10^7/mL) at 37°C and injected into a mold (D 4 mm, $H = 3$ mm). After solidification at room temperature, the cell/gel constructs were transferred to the 24-well culture plate and cultivated in the cell culture incubator (5% CO_2, 37°C) for 3–32 days. The EF phenomenon was observed ever since day 12 (Fig. 1). This demonstrating model is named EF-on-edge model.

MCG construction

Preparation of partially surface-crosslinked gelatin microspheres. Gelatin microspheres were fabricated with plain or Rhodamine B (Aldrich) prelabeled gelatin (Sigma) following a double emulsion method. Briefly, 10 mL ethyl acetate was mixed into 30 mL gelatin solution (0.1 g/mL in water) by stirring and the emulsion was further added into 60 mL soybean oil and stirred for 10 min. Gelatin microspheres were formed spontaneously in 300 mL precooled (−20°C) ethanol and rinsed with 1,4-dioxane/acetone in turn. After being air-dried, the microspheres (150–180 μm) were collected via standard sieves (80–100 mesh). A partial surface-crosslinking treatment was conducted on the selected microspheres via suspension in *N*-ethyl-*N*′-(3-dimethylaminopropyl) carbodiimide solution (in 90% ethanol) at 4°C for 12 h, followed by another suspension in PBS with trace amounts of glutaraldehyde at 4°C for 19 h. The products were washed in pure ethanol and dried in vacuum oven.

Acellular MCG construction. The partially surface-crosslinked gelatin microspheres were preequilibrated in PBS at 4°C overnight and then suspended in 2 wt% agarose solution (in PBS; solution/microsphere ratio, 1:0.2 mL/g) at 37°C. After injecting into a mold (<1 mm thick), the mixture was solidified by cooling down to below 25°C before a speed-controlled spontaneous dissolution of the encapsulated gelatin microspheres to create cavities inside the agarose gel

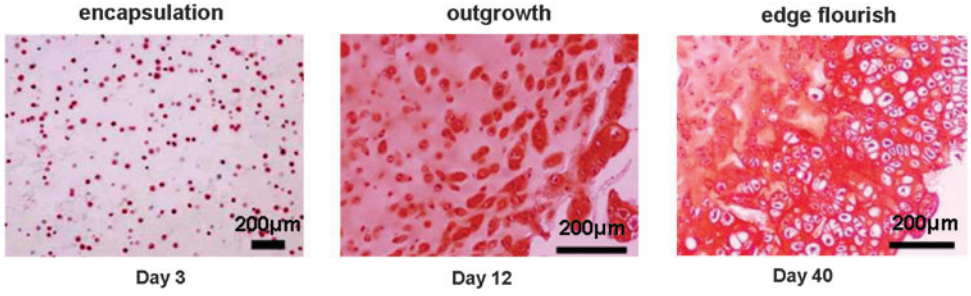

FIG. 1. Schematic and histological illustration of edge flourish (EF) phenomenon in EF-on-Edge model. The column panels from left to right indicate, in plain agarose hydrogel, cell seeding on day 3, cell outgrowth on day 12, and neo-tissue formation around the gel (EF effect) on day 40, respectively. The row panels from the top to the bottom are schematic illustration and histological indication of EF procedure, respectively. In histological indication, positive glycosaminoglycan (GAG) production is demonstrated with red Safranin-O stain. Color images available online at www.liebertonline.com/ten.

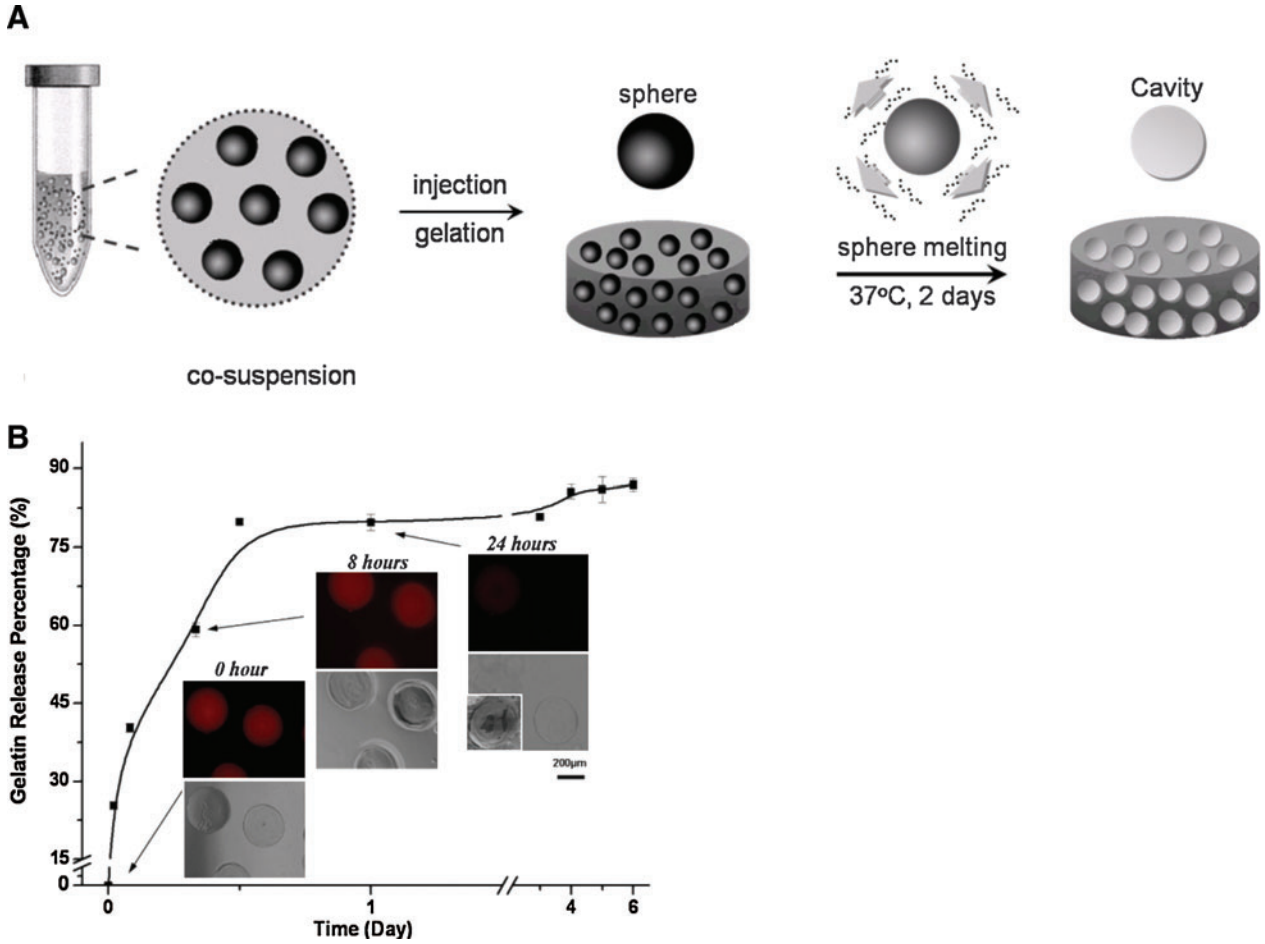

FIG. 2. (**A**) Schematic demonstration of construction of microcavitary hydrogel (MCG) model. (**B**) Kinetics of cavity creation quantified by amount of gelatin release percentage over 6 days and qualitative illustration of gradual dissolution of microspheres. Color images available online at www.liebertonline.com/ten.

bulk as illustrated in Figure 2A. The rhodamine-labeled gelatin (red) was employed to trace the dissolution of spheres and the residual gelatin in the construct was quantified by hydroxyproline test as shown in Figure 2B.

PTCC in cell-laden MCG system

Agarose-based MCG-PTCC model. Chondrocytes were cosuspended with partially surface-crosslinked gelatin microspheres in 2 wt% agarose solution as shown in Figure 3A. The final cell density in agarose constructs was $\sim 1\times10^7$/mL. The mixture was injected into a mold and it was solidified by the similar method as mentioned in MCG construction. As for control, conventional hydrogel constructs were prepared by encapsulating chondrocytes (cell density: 1×10^7/mL) without gelatin microspheres in agarose. The constructs were cultured in chondrocytes culture medium with shaking (60 rpm) in the cell culture incubator (5% CO_2, 37°C) for up to 32 days and the culture medium was changed every 2–3 days. The agarose MCG constructs were utilized to evaluate the overall performance of tissue regeneration.

The self-formation of microcavities by delayed dissolution of the coencapsulated microspheres is demonstrated in Figure 3B. The whole PTCC procedure is recorded and demonstrated in Figure 3C. Besides the encapsulated cells, to trace the fate of hydrogel component in PTCC system quantitatively, the agarose content of lyophilized cell-laden MCG constructs was measured by determining 3,6-anhydrogalactose content roughly according to Yaphe and Arsenault,[7] compared with that of the constructs without cavities. Using pure agarose as standard, the residual agarose content at given time points was calculated according to the following equation: agarose remaining percentage $= W_t/W_0$, where W_0 and W_t denote the relative weight of agarose at day 0 and other given time point, respectively. The result is indicated in Figure 3D.

Alginate-based MCG-PTCC model. The PTCC procedure was also practiced in alginate-based cell-laden MCG system. Chondrocytes were suspended in 1.2 wt% alginate solution and mixed with surface-crosslinked gelatin spheres to form MCG constructs. The final cell density in alginate constructs was $\sim 1\times10^7$/mL. The alginate MCG constructs were formed by dispensing the alginate-cell suspension dropwise (40 μL/drop) into a 102 mM calcium chloride solution using pipette. The constructs were cultured in the same conditions as the agarose constructs. Cells embedded in the alginate could be re-isolated without any harm using the alginate recovered chondrocytes method[7] and thus used for analysis of the gene expression of aggregated cells grown in the unconfined phase and scattered cells grown in the hydrogel phase.

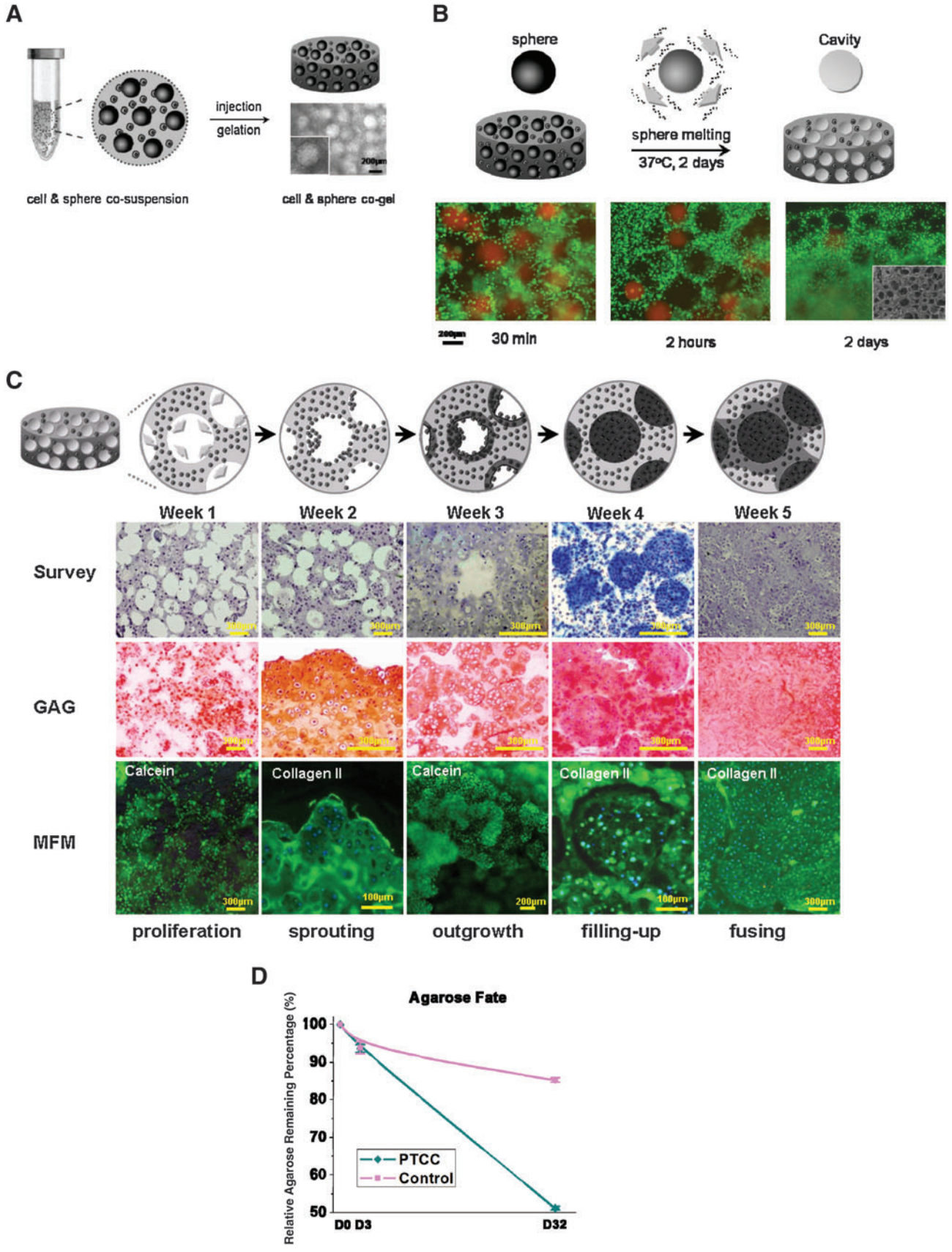
A
injection
gelation
cell & sphere co-suspension
cell & sphere co-gel
B
sphere
Cavity
sphere melting
37°C, 2 days
30 min
2 hours
2 days
C
Week 1
Week 2
Week 3
Week 4
Week 5
Survey
GAG
MFM
Calcein
Collagen II
Calcein
Collagen II
Collagen II
proliferation
sprouting
outgrowth
filling-up
fusing
D
Agarose Fate
Relative Agarose Remaining Percentage (%)
100
90
80
70
60
50
PTCC
Control
D0 D3
D32

RNA extraction

From EF-on-edge model. As described in the "Chondrocytes isolation, encapsulation, and EF determination" section, the constructs of EF-on-edge model were prepared, based on which the EF layer was separated from gel bulk by punching out the surface part from the gel construct. The top and bottom surfaces of the solid gel bulk were also carefully cut off as parts of the EF layer. The EF layer and gel bulk were thus distinguished and separated for subsequent RNA extraction using a combination of TRIzol® (Invitrogen) and RNeasy® Mini Plant Kit (Qiagen), as specifically reported by our group.[15]

From agarose-based MCG-PTCC model. As described in the "Agarose-based MCG-PTCC model" section, PTCC strategy was launched in agarose-based cell-laden MCG constructs. To extract RNA, the whole construct was homogenized and RNA from specimens was extracted using the combination of TRIzol (Invitrogen) and RNeasy Mini Plant Kit (Qiagen).[15] The acquired RNA samples (from cell-laden constructs) were treated with RNase-free DNase I and converted to cDNA for subsequent polymerase chain reaction (PCR) experiments.

From alginate-based MCG-PTCC model. As mentioned in the "Alginate-based MCG-PTCC model" section, PTCC strategy was also employed in alginate-based cell-laden MCG constructs. Before RNA extraction, alginate recovered chondrocytes method[7] was used to distinguish the cell islets induced by PTCC procedure from scattered cells/colonies remaining in the gel-bulk. When obvious cell aggregations could be observed using optical microscope, alginate-based MCG constructs were collected and dissolved in a buffer containing 55 mM sodium citrate and 0.15 M sodium chloride at pH 6.8, for 10 min at 4°C, to remove alginate and release scattered or aggregated cells. The resulting suspension of chondrocytes (mixture individual and aggregated cells) was filtered by a cell strainer (40 μm Nylon; BD Falcon). The aggregated chondrocytes on the strainer and the scattered cell in the filtrate were collected, respectively. These two populations of cells were centrifuged separately and then the cell pellets were washed before resuspending them in PBS. Accordingly the two distinct forms of chondrocytes were separated from each other and RNA was extracted by TRIzol (Invitrogen).

Real time polymerase chain reaction (RT-PCR)

For real-time quantitative PCR, the relative gene expression values were obtained from iQ™ qPCR system (Bio-Rad) and calculated with the comparative ΔΔCT (threshold cycle) method, as normalized to the housekeeping gene. All the real time polymerase chain reaction (RT-PCR) reagents used above were purchased from Promega. All the primers used are listed in Table 1, and all the oligonucleotides were synthesized by AIT Biotech.

Biochemical assays

"Live/Dead" dye staining (Molecular Probes, Invitrogen) was used to determine the viability of chondrocytes. The loaded viable cells were indicated with green fluorescent calcein. Biochemical assays were performed on the lyophilized cell-laden MCG constructs. The specimens were digested with 1 mL papain solution (0.3 mg/mL, mixed with 0.1 mM disodium ethylenediaminetetraacetic acid in 0.2 mM dithiothreitol) for 24 h. By centrifugation, the supernatant containing digested cell lysate was collected for measurement of cell numbers (via DNA quantification using Hoechst 33258 dye), collagen content (via hydroxyproline quantification), and glycosaminoglycan (GAG) content (with dimethylmethylene blue).

Histology

For histological evaluation, paraformaldehyde (4%)-preserved sample slices were stained with hematoxylin and eosin, Safranin-O, and Masson's trichrome dyes, respectively. Collagen II primary antibody (2 μg/mL in PBS; MAB8887; Chemicon) and anti-IgG (5 μg/mL in PBS; Alexa Fluor 488; Invitrogen) were utilized for collagen II staining, collagen I primary antibody (2 μg/mL, mouse monoclonal IgG; Santa Cruz Biotechnology) and anti-IgG (5 μg/mL; Alexa Fluor 543; Invitrogen) were utilized for collagen I staining, and neural cell adhesion molecule (NCAM) antibody with fluorescein conjugates (sc-7326 FITC; Santa Cruz Biotechnology) was applied for NCAM staining.

Scanning electron microscopy

Field emission scanning electron microscopy (JSM-6700F; Jeol) was used to examine the microstructure of MCG constructs. Briefly, the glutaraldehyde (2.5%)-preserved MCG constructs were treated with 1% OsO_4 at 4°C for 2 h, then

FIG. 3. Schematic and histological illustration of phase transfer cell culture (PTCC) strategy in cell-laden MCG model. (**A**) Schematic demonstration and optical microscopic illustration of fabrication and formation of "cell-and-sphere co-encapsulating gel" construct as the early step of MCG construction. (**B**) Achievement of cell-laden MCG construct: the row panels from the top to the bottom are schematic illustration and histological indication of cavity creation in cell-laden hydrogel bulk, respectively. The selected time points of detection are 30 min, 2 h, and 2 days, respectively. SEM micrograph is supplemented to illustrate cavities formed in gel bulk at time point of 2 days. (**C**) Demonstration of PTCC strategy and procedure in MCG model: the row panels from the top to the bottom are schematic illustration (top row) and histological indication (second through bottom row) of PTCC procedure. In the second row, hematoxylin and eosin stain was applied to survey the histological evolution, except for that in the "filling-up" image in which Masson's trichrome stain was applied to reveal positive collagen production in blue; in the third row, Safranin-O stain was applied to reveal positive GAG production in red; and in the bottom row, multiple fluorescence microscopy (MFM) was used and fluorescent 4′,6-diamidino-2-phenylindole stain was applied to position the cell nuclei in purple, simultaneously green fluorescent calcein stain was applied to image the "proliferation" and "outgrowth" processes, and immunohistochemical stain conjugating with green fluorescent chromophore was applied to image the "sprouting," "filling-up," and "fusing" processes with type II collagen as the primary antibody. (**D**) Graph of kinetics of agarose degradation in PTCC and Control sample quantified with relative agarose remaining percentage till 32 days. The curves are marked as cyan and magenta colors for PTCC and Control samples, respectively. Color images available online at www.liebertonline.com/ten.

Table 1. Polymerase Chain Reaction Primers Used in This Study

Genes	*Primer sequence (both 5′–3′)*[a]
GAPDH[14]	F: ACCCCTTCATTGACCTCCAC; R: ATACTCAGCACCAGCATCGC
HPRT1	F: GGACTTGAATCATGTTTGTG; R: CAGATGTTTCCAAACTCAAC
RPL4	F: CAAGAGTAACTACAACCTTC; R: GAACTCTACGATGAATCTTC
TBP1	F: AACAGTTCAGTAGTTATGAGCCAGA; R: AGATGTTCTCAAACGCTTCG
Collagen II[14]	F: GCTATGGAGATGACAACCTGGCTC; R: CACTTACCGGTGTGTTTCGTGCAG
Aggrecan[14]	F: CGAGGAGCAGGAGTTTGTCAAC; R: ATCATCACCACGCAGTCCTCTC
RhoA	F: AGCTGGGCAGGAAGATTATG; R: TGTGCTCATCATTCCGAAGA
Integrin β1	F: TGCCAAATCATGTGGAGAATGTAT; R: GTCTGTGGCTCCCCTGATCTTA
Sox9	F: GCTGGCGGATCAGTACCC; R: CGCGGCTGGTACTTGTAA
COMP	F: GGCACATTCCACGTGAACA; R: GGTTTGCCTGCCAGTATGTC

[a]F and R denote "forward" and "reverse" sequences, respectively.

dehydrated in gradient ethanol solutions, and further dried in vacuum overnight. Platinum was sputtered for scanning electron microscopy contrast.

Animal experimentation

All the animal experiments were performed under guidelines approved by the Institutional Animal Care and Use Committees, SingHealth, Singapore. Specimens with chondrocytes (agarose model) were implanted subcutaneously in the dorsum of athymic nude mice after 7–10 days culture *in vitro*. Briefly, the nude mice were anesthetized by Ketamine (40 mg/kg) and Diazepam (5 mg/kg) mixture and disinfected with 70% ethanol and iodine. Then two incisions were made on the back skin of each animal, and the specimens were implanted subcutaneously through each of the incisions. After suturing up, the animals were raised for 3 or 6 weeks and then euthanized by cervical dislocation after anesthetizing the mice. The embedded constructs were taken out from the subcutaneous tissue for bioanalysis. In total, 12 animals were used, each with two constructs inserted.

Statistical analysis

Biochemical data from cell-laden hydrogel constructs with cavities were compared with that obtained from cell-laden hydrogel constructs without cavities with equal incubation times using Student's *t*-test, with three specimens in each group. The significant level was set as $p < 0.05$. Results are reported as mean ± standard deviation.

Results

EF phenomenon

As highlighted in Figure 1, cellular outgrowth is visible after 12 days of culture in a simple cell-laden agarose hydrogel construct *in vitro*, and with further culturing till day 40, an abundant neo-tissue outgrowth is generated at the gel edge, forming a continuous scaffold-free phase, covering the entire outer surface of the construct. This phenomenon is recognized and defined as EF. The Safranin-O staining used in this typical EF-on-edge model revealed high cell proliferation and ECM production such as GAG in this outgrowth layer (Fig. 1).

Evaluation of the EF layer from EF-on-edge model

The EF phenomenon was evaluated by phenotypic evidences based on mRNA and protein level expressions. As depicted in Figure 4A, there is higher expression of *RhoA*, cellular connective proteins such as *COMP* and collagen type II, transcription factor *Sox 9*, and aggrecan in the cell colonies at the surface than those in the gel bulk at almost all time points investigated. In particular, highest expression of *RhoA*, collagen II, *Sox 9*, and aggrecan were recorded on day 18 for both surface and bulk cell colonies.

The secretion of the ECM was assessed by GAG and total collagen production as shown in Figure 4B. There was an increasing production of both GAG and total collagen at the gel surface and gel bulk from day 10 to 32. The production of GAG was slightly higher in the gel bulk than the gel surface, whereas total collagen production was much higher in gel surface than gel bulk on day 32.

Construction of acellular MCG

The observation of EF inspires the work of the PTCC system to generate multiple interfaces within the gel bulk via the MCG model, which render the EF effects from the outer edge of the gel construct to the inner surface of the cavities within the gel. The establishment of MCG model was clearly indicated by the prelabeled Rhodamin B fluorescence gelatin microspheres degradation, which was monitored both qualitatively (Fig. 3B) and quantitatively (Fig. 2B). The delayed dissolution of water-soluble gelatin microspheres was achieved by the precrosslinked treatment on the spherical surface layer and any dissolved gelatin molecules were released through the highly permeable gel network.

Construction of MCG-PTCC model

Figure 3 demonstrates the PTCC strategy and procedure in MCG model. It proceeds in four steps: (1) Therapeutic cells were cosuspended and then coencapsulated in agarose hydrogel together with gelatin microspheres that were fabricated with 200–400 μm diameter and lightly crosslinked in spherical surface layer as indicated in Figure 3A. (2) The hydrogel constructs coencapsulating cells and microspheres were incubated in a chondrocyte growth medium for a prolonged period of time. During the first 2 days or so, when the cells were settling down in gel bulk, the coencapsulated gelatin microspheres gradually dissolute off to create same sized cavities. The MCG model was established. The whole procedure was recorded and assessed by moni-

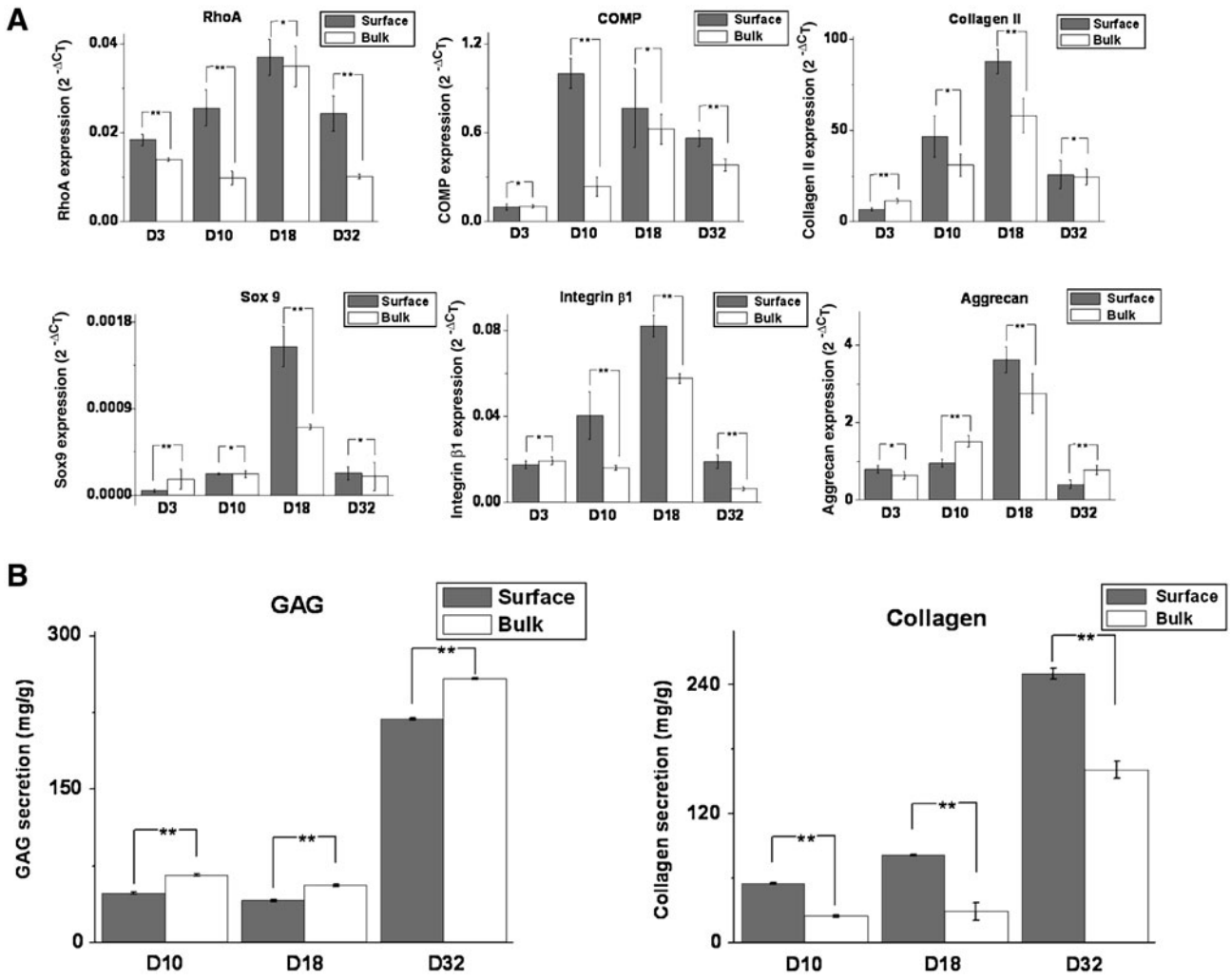

FIG. 4. (**A**) Analysis of the expression of relevant cartilaginous markers at transcriptional level from porcine chondrocytes in agarose gel surface and gel bulk by quantitative real-time polymerase chain reaction (PCR) ($n = 3$). The values represent the levels of expression relative to that of the internal control gene (GAPDH). Gray: cells at surface ($n = 3$); white: cells in bulk ($n = 3$). The values represent the means ± standard deviations. The selected time points of analysis are 3, 10, 18, and 32 days, respectively. *Differences between different constructs at the same culture time are not significant ($p > 0.05$); **differences between different constructs at the same culture time are significant ($p < 0.05$). (**B**) Graphical representations of the secretion of extracellular matrix in agarose gel surface and gel bulk. From left to right, the panel illustrates the secretion of GAG and total collagen, respectively, as a function of culture time at 10, 18, and 32 days. The values have been normalized by the dry weights of the gel surface and gel bulk and represent the means ± standard deviations. **Differences between different constructs at the same culture time are significant ($p < 0.05$).

toring the disappearance of prelabeled red Rhodamine B fluorescence in gelatin microspheres both qualitatively and quantitatively in Figures 3B and 2B, respectively. At the same time, the cells remained viable within the hydrogel as shown by calcein staining after 2 days in Figure 3B. (3) As the cultivation continued, EF phenomenon began to take place at gel-cavity interface at about 15 days; following which, trans-phase sprouting and outgrowth of cell colonies gradually developed into scaffold-free neo-tissue islets and eventually filled up the cavities with densely populated cells and endogenous ECMs that both showed *bona fide* morphologies as those in the native (tissue) counterparts. This process is shown schematically and histologically in the first and second rows of Figure 3C through hematoxylin and eosin and Masson's trichrome staining, which stained the islets blue. In the third row, Safranin-O stain applied has stained greater area red; and in the bottom row, multiple fluorescence microscopy was applied, indicating the high viability of the cells throughout the neo-tissue islet generation and the increasing total collage production (collagen type I was also tested and the results were negative) from the cells in the MCG construct. (4) With further cultivation, these scaffold-free islets act as neo-tissue cores and demonstrated strong tendency of expansion to fuse with each other and also with isolated cells or colonies remaining in gel bulk so that a piece of maximally scaffold-free three-dimensional (3D) macroscopic tissue was tangibly engineered.

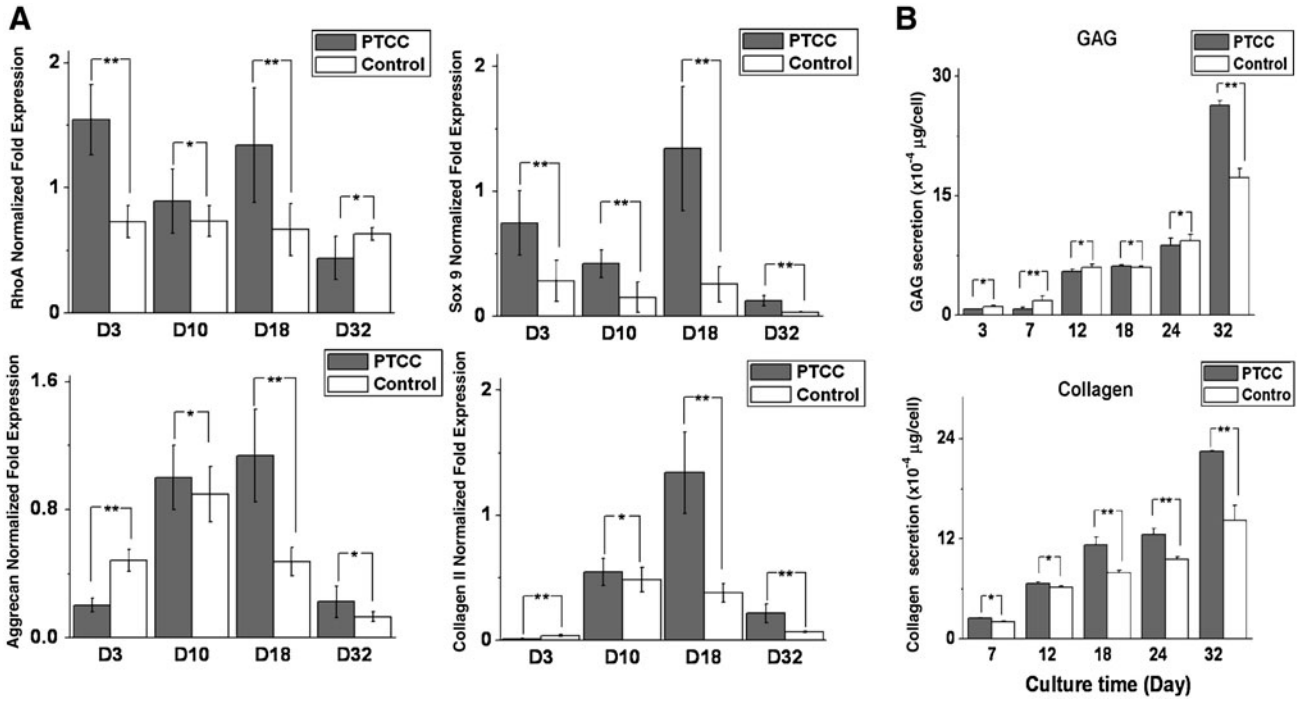

FIG. 5. Practicable illustration of the superiority of MCG employing PTCC strategy ("PTCC" samples), in contrast with plain agarose hydrogel without alteration ("Control" samples) *in vitro* and *in vivo*. (**A**) Analysis of the expression of relevant cartilaginous markers at transcriptional level from porcine chondrocytes in PTCC samples and Control samples, adopting agarose hydrogels, by quantitative real-time PCR ($n = 3$). The values represent the levels of expression relative to that of two internal control genes (HPRT and RPL4). Gray: cells in PTCC samples ($n = 3$); white: cells in Control samples ($n = 3$). The values represent the means ± standard deviations. The selected time points of analysis are 3, 10, 18, and 32 days, respectively. (**B**) Investigation of the secretion of extracellular matrix in PTCC samples and Control samples. The row panels from the top to the bottom illustrate the secretion of GAG and total collagen, respectively, as a function of culture time at 3, 7, 12, 18, 24, and 32 days. *Differences between different constructs at the same culture time are not significant ($p > 0.05$); **differences between different constructs at the same culture time are significant ($p < 0.05$).

Gene expression and ECM production in MCG-PTCC model

Comparison between the MCG-PTCC model and a plain hydrogel model was made based on the mRNA and protein expression. As shown in Figure 5, there are higher expressions of *RhoA*, *Sox 9*, aggrecan, and collagen type II in cells encapsulated in the MCG-PTCC model compared with the control group, and at the protein level, GAG and total collagen production are also greater in the MCG-PTCC model.

Further examination is conducted in an alginate hydrogel-based MCG-PTCC model from which, by dissolving the alginate construct with sodium citrate, the neo-tissue islets in cavities and the scattered cells remaining in gel phase were separately harvested and their gene expression profiles were revealed, respectively, as shown in Figure 6. These results again confirmed the conclusions that proliferation profile and the maintenance of chondrocytic phenotype are more superior in the EF layer.

Fate of agarose in MCG-PTCC system

With respect to the dissolution of hydrogel scaffolding material, the results in Figure 3D showed the kinetics of agarose degradation, quantified with relative agarose remaining percentage till 32 days. The clearance of the polysaccharides exhibited a linear molecular release profile.

In vivo *evaluation of MCG-PTCC model*

The subcutaneous implantation of MCG constructs in nude mice were harvested and evaluated after a few weeks of cultivation. There were higher secretions of both GAG and collagen type II throughout the MCG construct giving rise to a continuous phase of ECM among the cells unlike those in the plain hydrogel control as indicated by the immunostaining in Figure 7. Collagen type I was also tested and the results were negative.

Discussion

EF phenomenon

After a long-term culture of cell-laden hydrogel constructs *in vitro*, in contrast with the modest cell growth appearing in gel bulk, there was an abundant neo-tissue outgrowth along the gel edge, showing microscopic flourish of both cell proliferation and ECM production. This phenomenon has been observed in various individual systems that are all made of hybridizations between non(typical) anchorage-dependent cells and noncell-adhesive hydrogels. This setting implies the preconditions for emergence of EF phenomenon: (1) the 3D cell-laden microenvironment in hydrogel bulk lacks focal adhesive functionality for cell attachment; and (2) being entrapped and confined in the framework-lattice of hydrogel

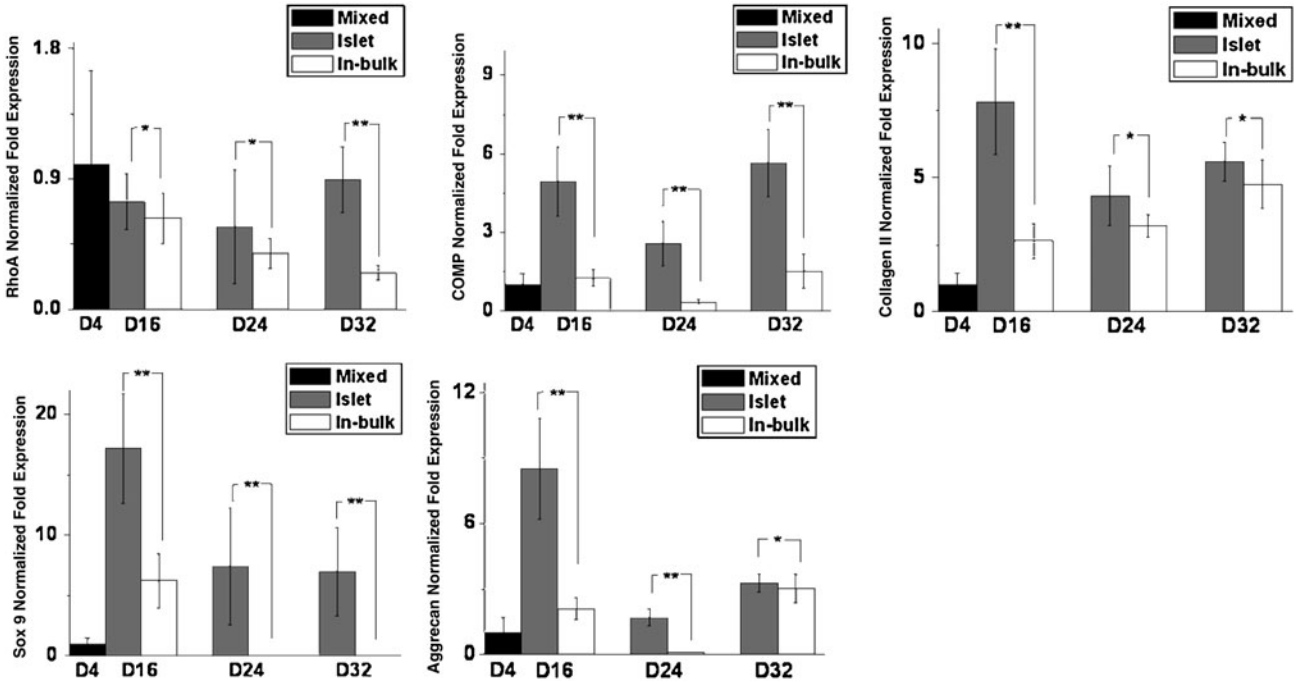

FIG. 6. Analysis of the expression of relevant cartilaginous markers at transcriptional level from porcine chondrocytes in PTCC samples, adopting alginate hydrogels for distinguishing between aggregated cell islets and individual cells in bulk, by quantitative real-time PCR ($n = 3$). The values represent the levels of expression relative to that of two internal control genes (HPRT and RPL4). Black: mixed cells at the initial stage ($n = 3$); gray: aggregated cell islets ($n = 3$); white: cells in gel bulk ($n = 3$). The values represent the means ± standard deviations. The selected time points of analysis are at 4 (initial stage), 16, 24, and 32 days, respectively. *Differences between different constructs at the same culture time are not significant ($p > 0.05$); **differences between different constructs at the same culture time are significant ($p < 0.05$).

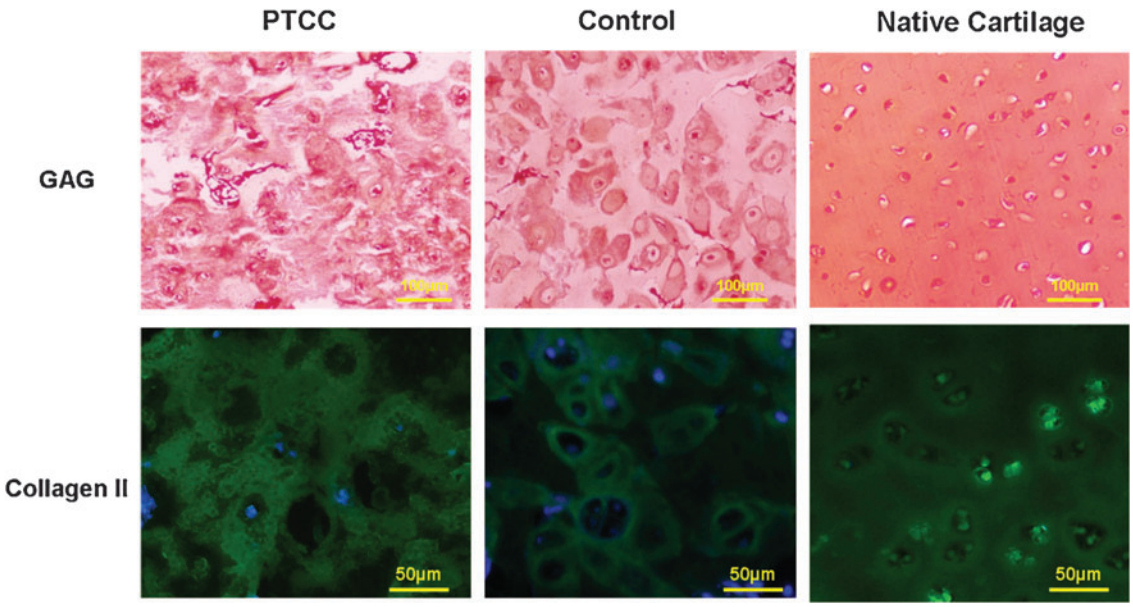

FIG. 7. Histological evaluation of PTCC samples cultured *in vivo* for 40 days in contrast with Control samples and native cartilage (left, center, and right column, respectively), both PTCC and Control samples adopting agarose hydrogel. In the first row, Safranin-O stain was applied to reveal positive GAG production in red; in the second row, immunohistochemical stain conjugating with green fluorescent chromophore was applied to image the samples with primary antibody of type II collagen. Color images available online at www.liebertonline.com/ten.

scaffold where there is a lack of focal adhesive settlement, the cells are still capable of maintaining high viability and proliferative tendency. Among these two implications, precondition (1) fits the property of noncell-adhesive hydrogels including photo-crosslinked polyethylene glycol-based gels and neutrally or negatively charged thermocure polysaccharide gels such as agarose, gellan gum, and alginate; precondition (2) generally refers to non(typical) anchorage-dependent cells such as chondrocytes and numerous cell species among endodermal lineages. When both conditions were applied to our cell-encapsulated hydrogel system, cell colonies located deep in the gel bulk would experience limited growth due to the physical constraint by the scaffold framework, whereas those located adjacent to the edge of the gel construct would continuously expand toward the gel surface and ultimately sprout out to form the EF layer on the interface as indicated in Figure 1.

To further investigate the properties of the cells in the EF layer, chondrocytic markers and ECM protein expressions were tested. The greater expression of *RhoA* at surface layer reflects a higher proliferative profile of the local cell population that ultimately constitutes the EF *per se*. In addition, the maintenance of chondrocytic phenotype also proves better in the cells residing in surface layer based on superior gene expression and proteinic yields of the cartilage markers including chondrogenic transcription factor (*Sox9*), cartilaginous collagen (type II), and proteoglycan (aggrecan/GAG). ECMs. Further culturing of the MCG construct revealed the strong tendency of expansion from the islets, which led to fusion of these islets with one another or scattered cells, giving rise to a maximally scaffold-free 3D macroscopic tissue that showed *bona fide* morphologies similar to native cartilage (Fig. 3C). The chondrocytic markers used in the EF evaluation were tested on the cells in our MCG-PTCC and it confirmed that this system is indeed superior over the plain hydrogel model. Phenotypic markers such as collagen II and GAG were preserved, and also there is neo-tissue islets formation as indicated in comparison between islets and scattered cells (Figs. 5 and 6). Collectively, all these results demonstrated the feasibility of our system in fabrication and maintenance and even enhancement of viability and phenotype of the employed chondrocytes.

It is also notable that the gelatin microspheres used in this PTCC strategy is in the range of few hundreds of microns and therefore maintains injectability of our MCG-PTCC system. The clearance of agarose scaffolding material, given the physical crosslinking in this gel, the 3D network would experience a gradual disentanglement under growing pressure from the expanding neo-tissue islets and ends up with a removal via linear molecular release. This, at a certain level, addresses the requirement on degradation of the scaffold used in the field of tissue engineering and regenerative medicine and eventually leaves a nearly scaffold-free neo-tissue.

Setup of MCG-PTCC system

The results and performances in the EF-on-Edge modeling system have inspired the work of the PTCC system to generate multiple interfaces within the gel bulk via the MCG model, which renders the EF effects from the outer edge of the gel construct to the inner surface of the cavities inside the gel. With that, the EF effect can occur inside the hydrogel construct, translating it to a practical methodology for engineering applications. It also converts the role of hydrogel from a noncell-adhesive substrate to a productive nursery for cells to grow (Fig. 3A). It is important that the ratio of weight of microspheres (porogens) to the weight of hydrogel does not exceed 0.3:1 as too many microcavities within the hydrogel would compromise mechanical properties of the construct and result in difficulties during handling. Also, the size of the microcavities should be within 100–500 μm. Gel constructs with cavities smaller than 100 μm cannot be sufficiently distinguished from common gel systems because they are also porous in nature. As the EF layer is typically six to eight cell layers thick, which is ~200–250 μm, cavity size should not be larger than twice of the EF layer thickness (500 μm) because such large cavities cannot be fully filled up by outgrowing cell colonies.

The results in Figure 3A–C have proven the feasibility of the MCG-PTCC system. The 2 days' delayed dissolution of water-soluble gelatin microspheres was obtained by the precrosslinking treatment in spherical surface layer. The dissolved gelatin molecules were released off through the well-permeable gel network, which created microsized cavities within the hydrogel construct. The outgrowth from the edges created within the hydrogel would later develop into scaffold-free neo-tissue islets when all the cavities were filled up by densely populated cells and their endogenous

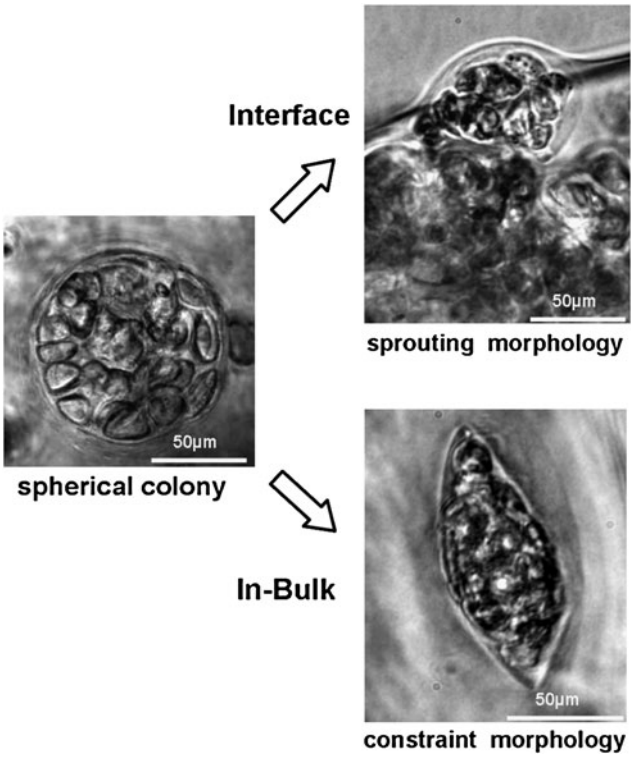

FIG. 8. Optical microscopic illustration of cell interaction in EF-on-Edge model. The column panels from left to right indicate, in plain agarose hydrogel, cells forming spherical colonies, and the subsequent different fate of the colonies located in either the favoring interface (in the upper row) or the obstructive bulk (in the lower row).

Mechanisms of PTCC in MCG construct

As the design of MCG-PTCC system is an adoption of EF phenomenon, mechanism studies on initiation of EF phenomena such as medium diffusion, gelatin presence, and interfacing mechanics are carried out with the EF-on-Edge.

The variable of medium diffusion in hydrogel is always a vital factor for all types of cell culture. It is excluded from being a dominant reason for initiation of EF effect, though it remains a substantial factor responsible for the development of EF outgrowth thereafter because of the consistent outcomes yielded from both EF-on-Edge model and MCG-PTCC system. In the EF-on-Edge model, EF arises at direct exposure to ambient medium, whereas in the MCG-PTCC system, PTCC proceeds inside gel body barely exposing to the permeated medium in cavity. From the comparable results (Figs. 1 and 3C) in these contrasting cases, it proves that medium diffusion has no significant role in the initiation of EF effect and PTCC phenomenon. In fact, a consensus has long existed among hydrogel users: as long as the construct is made small enough the generally well-permeable hydrogels do not hinder molecular-level transportation therein.[28] This position is further confirmed by an additional experiment when serum concentration varies in formulation of culture medium; both the EF-on-Edge and the PTCC in MCG are still capable of happening only with a matter of being sooner or slower.

The potential contribution of soluble gelatin to initiation of PTCC in MCG is regarded as negligible. This is based on two facts: first, in the EF-on-Edge model, the EF phenomenon occurs without any involvement of gelatin (Fig. 1); second, in the MCG-PTCC system, the dissolution and clearance of gelatin component is accomplished within 2–7 days (Fig. 2B), which is much earlier than the initiation of trans-phase cell growth on day 15 (Fig. 3C). Further, the morphological evaluations of the outgrowing cell colonies showed that the cells were not in a spread-out conformation. Although chondrocytes is a nontypical anchorage-dependent species, it still reserves a preference for focal adhesion if condition permits. If gelatin had played a critical role in the initiation of trans-phase growth of cells residing adjacent to gel-cavity interface, it would induce focal adhesion in these cell populations because it is a potent cell-adhesive protein. However, experimental outcomes do not indicate any commitment of focal adhesion in chondrocytes (as shown in Figs. 1 and 3C). Putting all these evidences together, gelatin microspheres only played the role as porogen for establishment of MCG construct, and any cell growth contributed by gelatin is minimal.

The nature of EF phenomena is attributed as a biomechanical response between hydrogel scaffold and the cell colonies inside. An asymmetric compression exerted by hydrogel frame orientates the growing direction of the cell colonies located at the surface of hydrogel toward the outside. When scattered cells are seeded in the lattice of hydrogel framework, the polymeric backbone of gel frame is flexible enough to allow cells to proliferate into colonies. The growth continues until the colony reaches a certain critical size that is confined by maximal flexibility of employed materials. Along with the expansion of cell colonies, the resisting pressure by gel framework increases accordingly. If the cell colonies were encapsulated deep in gel bulk, it would receive symmetric compressions from the surroundings. When the pressure increases and manages to balance the expanding force of cell division, further cell proliferation is mechanically prohibited. On the other hand, cell colonies at the surface layer of hydrogel experienced an asymmetric compression from the surrounding hydrogel as the local compressive modulus sharply decreases with the reducing material density from the bulk side toward interface. The cell colonies residing there would receive lower pressure from the interface side and it is not sufficient to counteract the expanding force of cell division. Driven by this outward mechano-orientation, morphology of outgrowth of cell colonies from the surface layer of hydrogel is thus initiated. Therefore, cell colonies may appear in spherical or spindle shape depending on their local mechano-homogeneity, as shown in Figure 8. In agarose gel–based working conditions that are particularly adopted in this model study, a "critical thickness" of the surface layer for EF occurrence therein is observed as a depth varying between 100 and 200 μm under the interface. Below this depth is regarded as the gel "bulk," where it is free of EF-on-Edge. This finding suggests that in the MCG-PTCC system, by manipulating the intercavitary distance below the "critical thickness," a completely "bulk-free" construct could be produced in which all-pervasive EF effects would enable a full-scale histogenesis followed by comprehensive neo-tissue occupation (proven both *in vitro* and *in vivo* as indicated in Figs. 3 and 7).

Conclusion

In conclusion, inspired by a coincidental captured EF phenomenon during routine work with cell-laden hydrogels, an innovative 3D cell cultural strategy PTCC was designed and practiced within a jointly invented MCG system, mediated by an interfacing mechanoresponsive nature of the processing, and also translational trials were accomplished both *in vitro* and *in vivo*. By this invention, new doors will be opened to engineering histogenesis in hydrogel-based scaffolding system. It may potentially benefit the related explorations in engineered regenerative medicine.

Acknowledgment

The work was financially supported by grant AcRF Tier 1 RG 64/08, Ministry of Education, Singapore and NMRC/EDG/1001/2010, National Medical Research Council, Singapore.

Disclosure Statement

No competing financial interests exist.

References

1. Bruck, S. Aspects of three types of hydrogels for biomedical applications. J Biomed Mater Res **7,** 387, 1973.
2. Kloxin, A., Kasko, A., Salinas, C., and Anseth, K. Photodegradable hydrogels for dynamic tuning of physical and chemical properties. Science **324,** 59, 2009.
3. Farndale, R., Buttle, D., and Barrett, A. Improved quantitation and discrimination of sulphated glycosaminoglycans by use of dimethylmethylene blue. Biochim Biophys Acta **883,** 173, 1986.
4. Freed, L., Hollander, A., Martin, I., Barry, J., Langer, R., and Vunjak-Novakovic, G. Chondrogenesis in a cell-polymer-bioreactor system. Exp Cell Res **240,** 58, 1998.

5. Kim, Y., Sah, R., Doong, J., and Grodzinsky, A. Fluorometric assay of DNA in cartilage explants using Hoechst 33258. Anal Biochem **174,** 168, 1988.
6. Masuda, K., Sah, R., Hejna, M., and Thonar, E. A novel two-step method for the formation of tissue-engineered cartilage by mature bovine chondrocytes: the alginate-recovered-chondrocyte (ARC) method. J Orthop Res **21,** 139, 2003.
7. Yaphe, W., and Arsenault, G. Improved resorcinol reagent for the determination of fructose, and of 3, 6-anhydrogalactose in polysaccharides. Anal Biochem **13,** 143, 1965.
8. Chang, N., Yeh, M., and Jhung, Y. Fabricating PLGA Sponge Scaffold Integrated with Gelatin/Hyaluronic Acid for Engineering Cartilage, Bioengineering Conference, IEEE 35th Annual Northeast, 2009.
9. Ronzière, M.C., Roche, S., Gouttenoire, J., Démarteau, O., Herbage, D., and Freyria, A.M. Ascorbate modulation of bovine chondrocyte growth, matrix protein gene expression and synthesis in three-dimensional collagen sponges. Biomaterials **24,** 851, 2003.
10. Cui, W., Li, X., Xie, C., Zhuang, H., Zhou, S., and Weng, J. Hydroxyapatite nucleation and growth mechanism on electrospun fibers functionalized with different chemical groups and their combinations. Biomaterials **31,** 4620, 2010.
11. Hutmacher, D.W., Ekaputra, A.K., Zhou, Y., and Cool, S. Composite electrospun scaffolds for engineering tubular bone grafts. Tissue Eng Part A **15,** 3779, 2009.
12. Ameer, G., Mahmood, T., and Langer, R. A biodegradable composite scaffold for cell transplantation. J Orthop Res **20,** 16, 2002.
13. Freed, L., Marquis, J., Nohria, A., Emmanual, J., Mikos, A., and Langer, R. Neocartilage formation *in vitro* and *in vivo* using cells cultured on synthetic biodegradable polymers. J Biomed Mater Res **27,** 11, 1993.
14. Jefferies, D., Farquharson, C., Thomson, J., Smith, W., Seawright, E., McCormack, H., and Whitehead, C. Differences in metabolic parameters and gene expression related to Osteochondrosis/Osteoarthrosis in pigs fed 25-hydroxyvitamin D 3. Vet Res **33,** 383, 2002.
15. Wang, C., Hao, J., Zhang, F., Su, K., and Wang, D. RNA extraction from polysaccharide-based cell-laden hydrogel scaffolds. Anal Biochem **380,** 333, 2008.
16. Wang, C., Gong, Y., Zhong, Y., Yao, Y., Su, K., and Wang, D. The control of anchorage-dependent cell behavior within a hydrogel/microcarrier system in an osteogenic model. Biomaterials **30,** 2259, 2009.
17. Yeh, J., Ling, Y., Karp, J., Gantz, J., Chandawarkar, A., Eng, G., Blumling Iii, J., Langer, R., and Khademhosseini, A. Micromolding of shape-controlled, harvestable cell-laden hydrogels. Biomaterials **27,** 5391, 2006.
18. Fisher, J., Jo, S., Mikos, A., and Reddi, A. Thermoreversible hydrogel scaffolds for articular cartilage engineering. J Biomed Mater Res **71,** 268, 2004.
19. Rice, M., and Anseth, K. Encapsulating chondrocytes in copolymer gels: bimodal degradation kinetics influence cell phenotype and extracellular matrix development. J Biomed Mater Res **70,** 560, 2004.
20. West, J., and Hubbell, J. Polymeric biomaterials with degradation sites for proteases involved in cell migration. Macromolecules **32,** 241, 1999.
21. Komura, M., Komura, H., Kanamori, Y., Tanaka, Y., Suzuki, K., Sugiyama, M., Nakahara, S., Kawashima, H., Hatanaka, A., and Hoshi, K. An animal model study for tissue-engineered trachea fabricated from a biodegradable scaffold using chondrocytes to augment repair of tracheal stenosis. J Pediatr Surg **43,** 2141, 2008.
22. Tan, H., Chu, C.R., Payne, K.A., and Marra, K.G. Injectable *in situ* forming biodegradable chitosan–hyaluronic acid based hydrogels for cartilage tissue engineering. Biomaterials **30,** 2499, 2009.
23. Xie, J., Ihara, M., Jung, Y., Kwon, I.K., Kim, S.H., Kim, Y.H., and Matsuda, T. Mechano-active scaffold design based on microporous poly (L-lactide-co-epsilon-caprolactone) for articular cartilage tissue engineering: dependence of porosity on compression force-applied mechanical behaviors. Tissue Eng **12,** 449, 2006.
24. Yoo, H.S., Lee, E.A., Yoon, J.J., and Park, T.G. Hyaluronic acid modified biodegradable scaffolds for cartilage tissue engineering. Biomaterials **26,** 1925, 2005.
25. Merrill, E., Salzman, E., Wan, S., Mahmud, N., Kushner, L., Lindon, J., and Curme, J. Platelet-compatible hydrophilic segmented polyurethanes from polyethylene glycols and cyclohexane diisocyanate. Trans Am Soc Artif Intern Organs **28,** 482, 1982.
26. Peppas, N., Hilt, J., Khademhosseini, A., and Langer, R. Hydrogels in biology and medicine: from molecular principles to bionanotechnology. Adv Mater **18,** 1345, 2006.
27. Tanahashi, K., and Mikos, A. Cell adhesion on poly (propylene fumarate-co-ethylene glycol) hydrogels. J Biomed Mater Res **62,** 558, 2002.
28. Lin, C.C., and Anseth, K.S. PEG hydrogels for the controlled release of biomolecules in regenerative medicine. Pharm Res **26,** 631, 2009.

Address correspondence to:
Dong-An Wang, Ph.D.
Division of Bioengineering
School of Chemical and Biomedical Engineering
Nanyang Technological University
70 Nanyang Drive, N1.3-B2-13
Singapore 637457
Singapore

E-mail: dawang@ntu.edu.sg

Received: April 12, 2010
Accepted: July 7, 2010
Online Publication Date: August 24, 2010